

Palladium Deposits on a Single Crystalline Cr₂O₃(0001) Surface

K. Wolter, H. Kuhlenbeck, and H.-J. Freund*

Fritz-Haber-Institut der Max-Planck-Gesellschaft Faradayweg 4-6, D-14195 Berlin-Dahlem, Germany

Received: December 31, 2001; In Final Form: March 29, 2002

Palladium deposits on a single crystalline Cr₂O₃(0001) film grown on Cr(110) have been studied under ultrahigh vacuum conditions. The growth mode at two different temperatures (90 and 300 K) was investigated using infrared reflection absorption spectroscopy of the probe molecule CO. The reduction of the amount of CO adsorbed on the oxide surface measured by the decrease of the CO stretching signal intensity was used to extract information about the surface area covered by the palladium deposits. The shape, fine structure, and half-width of the infrared absorption bands in the stretching frequency region of CO molecules bound to the palladium aggregates provides information about the morphology of the deposits. Additionally, the palladium induced attenuation of the phonon signals of the Cr₂O₃(0001) film has been studied applying HREELS. At 90 K, the palladium grows in two-dimensional islands which cover the entire oxide surface after deposition of one monolayer equivalent. If the palladium is deposited at a sample temperature of 300 K, the islands are three-dimensional but with a low aspect ratio. The changes of the structure of the deposits with increasing temperature are studied by infrared reflection absorption spectroscopy using the probe molecule CO and thermal desorption spectroscopy of CO. Upon an increase in the temperature, the crystallinity of the disordered particles grown at 90 K increases. Between 300 and 500 K, no structural changes are observed. At temperatures above 600 K, the palladium-induced signal vanishes in the infrared spectra. We suppose that the palladium diffuses into the substrate.

1. Introduction

The growth of metals on oxide surfaces has become a widely studied topic in surface physics and chemistry.^{1–4} The behavior of these systems toward chemical reactions does not only depend on the type of involved materials but also on the morphology and size of the metal particles. Most of the studies on single crystalline supports were performed using TiO₂, MgO, Al₂O₃, or ZnO substrates, whereas only a few studies for chromium oxide substrates have been reported. An overview can be found in ref 1. Chromium oxide has been used as a substrate for the deposition of Na,^{5,6} K,^{14,15} Mg,¹⁸ Cu,¹³ and Au.¹⁶ The investigation of Na on the Cr₂O₃(0001) surface revealed a strong chemical interaction of the sodium with the surface including metal–substrate charge transfer as might be expected for an alkali metal.^{5,6} Similar results were found for Mg,¹² Cu¹³ and Au¹⁶ show weaker interactions. Palladium is expected to be more similar to the latter than to alkali metal because the heat of palladium oxide formation is less negative than that for chromium oxide formation.⁷ We would like to compare the behavior of Pd deposits on Cr₂O₃(001) with that of Pd on Al₂O₃(0001) reported earlier.

Although Al₂O₃(0001) is rather inert, Cr₂O₃(0001) has some interesting properties with respect to adsorption and reaction.^{6,9–11} CO₂ for example has been shown to be activated by the Cr₂O₃(0001) surface to form a bent CO₂^{δ-} species.⁸ If small metal particles are deposited onto the chromium oxide, interesting new composite chemical properties may be generated. For instance, the particles may be used to activate hydrocarbons as a reaction partner for molecules activated on the chromia surface. Because these reactions would have to be taking place by spill-over, the

interfacial region between metal particles and the oxide support is important. Thus, metal particles sizes will play an important role.

On our way to the study of reactions, we report here as a first investigation on the growth of palladium clusters on a Cr₂O₃(0001) surface at two different temperatures. Also, the thermal stability of the Pd aggregates on the Cr₂O₃(0001) surface was investigated. We use CO as a probe molecule to study structure, morphology, and temperature-induced effects employing Fourier transform IR spectroscopy.

2. Experimental Section

The experiments have been performed in an ultrahigh vacuum apparatus with a base pressure of 2×10^{-10} Torr. The system contains a preparation chamber which is equipped with an Omicron 4 grid LEED system to check the surface order by LEED and its chemical constitution by Auger electron spectroscopy. Additionally, the preparation chamber contains a quadrupole mass spectrometer and a specially designed doser system in order to perform the thermal desorption measurements. Palladium is evaporated from a rod via electron bombardment using a commercial evaporator (Focus EFM 3T). The deposition rate was determined ex situ by a quartz microbalance to be about 1.3 Å per minute. IRAS measurements are performed using a modified Mattson RS-1 FTIR spectrometer. The IR light is generated by a global and after passing the interferometer focused onto the sample. The interferometer is mounted in a homemade steel chamber which is evacuated to 10^{-3} Torr. The light passes through viton-O-ring sealed KBr-windows before and after reflection at the sample surface. It is detected with a liquid-nitrogen-cooled MCT detector placed in a detector chamber which is flushed with dry nitrogen.⁶ All single beam

* To whom correspondence should be addressed. Fax: +49 30 8413-4101. E-mail: freund@fhi-berlin.mpg.de.

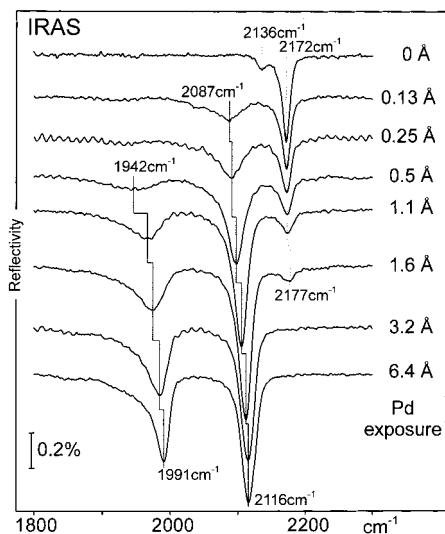


Figure 1. Infrared reflection absorption spectra of 10 L of CO adsorbed at 90 K on $\text{Cr}_2\text{O}_3(0001)/\text{Cr}(110)$ as a function of Pd exposure at 90 K.

spectra of this work were recorded with a spectral resolution of 2 cm^{-1} accumulating 500 scans for each spectrum. The reflectivity spectra were calculated from the single beam spectra of the clean and the adsorbate-covered surfaces. Afterward, they were baseline corrected. The HREELS measurements were performed using a VSI Delta 0.5 instrument with a theoretical resolution limit of 0.5 meV ($\sim 4\text{ cm}^{-1}$). All spectra shown have been recorded in specular reflection geometry with an incident angle of 65° and a primary electron energy of 5 eV . The count rates as well as the resolution depend strongly on the amount of deposited palladium because the increasing roughness of the surface leads to a broadening of the angular distribution of the reflected electron beam. The resolution obtained for the clean $\text{Cr}_2\text{O}_3(0001)$ surface is 16 cm^{-1} with a count rate of about 300 kHz in the elastic signal. Upon deposition of palladium, the resolution decreases to 50 cm^{-1} and count rates of $30\text{--}50\text{ kHz}$.

The chromium oxide film with (0001) orientation is prepared by oxidation of a clean $\text{Cr}(110)$ single-crystal surface according to well-known recipes.^{5,9,10,17,18} The thickness of the oxide film has been estimated to be about 40 \AA . The surface is terminated by a half-filled chromium-ion double layer in order to compensate for the “polar” character of the surface.^{17–19}

3. Growth of the Palladium Particles

3.1. Deposition at 90 K. Figure 1 shows infrared spectra of the stretching frequency region of CO adsorbed on $\text{Cr}_2\text{O}_3(0001)$ with different amounts of deposited palladium. The dosage of 10 L corresponds to saturation coverage at the measurement temperature of 90 K. The upper spectrum in Figure 1 exhibits data of CO on the clean $\text{Cr}_2\text{O}_3(0001)$ surface. The two signals in the spectrum originate from two different CO species on the surface which were investigated previously experimentally and theoretically.²⁰ The peak at 2136 cm^{-1} was assigned to a weakly bound physisorbed species ($E_a = 28\text{ kJ/mol}$), whereas the signal at 2171 cm^{-1} stems from weakly chemisorbed CO ($E_a = 45\text{ kJ/mol}$).²⁰ From previous ARUPS and NEXAFS measurements, it was concluded that the CO molecular axis is strongly inclined with respect to the surface normal.^{9,10} This result was supported by SCF-cluster calculations which found two CO species with different inclination angles.²⁰ The smaller tilt of the chemisorbed species leads to a higher infrared absorption cross section due to a higher dynamical dipole moment perpendicular to the surface.²¹

After deposition of a small amount of palladium onto the surface, the adsorption of CO leads to the appearance of a new absorption band at 2087 cm^{-1} . It is attributed to CO which is bound linearly (on-top) to the palladium particles.^{22–24} With increasing palladium coverage, the intensity of this signal increases and moves up to 2116 cm^{-1} . Starting from 0.5 \AA coverage, an additional absorption band appears at 1940 cm^{-1} which can be attributed to bridge-bonded CO on the palladium particles.^{22–24} With increasing palladium coverage, this signal moves to 1991 cm^{-1} . Parallel to the increase of the intensity of the CO signals originating from adsorption onto the palladium particles, the intensity of the absorption bands of CO adsorbed on the chromium oxide decreases. The band which is due to the physisorbed species disappears already after deposition of 0.13 \AA palladium. In contrast to this, the intensity of the band of the chemisorbed CO on the chromium oxide decreases more slowly. At a palladium coverage of 3.2 \AA , the band has disappeared. At this coverage, the palladium fully covers the oxide surface so that no adsorption sites are available for CO molecules. Because a thickness of 2.2 \AA corresponds to one monolayer of palladium, this points toward a high density of islands which eventually coalesce. As shown below, already at low Pd coverages, small islands are formed. The decrease of the intensity of the band of physisorbed CO cannot be understood on the basis of a site blocking by the palladium particles alone. It is conceivable that the palladium particles influence surrounding parts of the oxide surface. The theoretical calculation on the CO adsorption showed that the relaxation of the outermost oxide layers has a strong influence on the binding energy of the CO molecules.²⁰ We can speculate that the relaxation might be locally influenced by the deposited palladium. At low palladium coverage, the metal seems to be spread all over the surface in small nuclei, and formation of large aggregates is slow. This could explain the strong influence of small amounts of palladium onto the amount of physisorbed CO on the oxide surface.

The palladium coverage dependent changes in the ratio of the numbers of the linear and bridge-bonded CO molecules on the palladium particles can also provide information about the morphology of the deposits. At very low palladium coverages, the particles are so small that suitable sites for bridge-bonded CO molecules do not exist, whereas on large particles, such sites do exist and are preferentially occupied by the CO molecules. In the spectra in Figure 1, starting at a palladium coverage of about 0.5 \AA , a signal of bridge bonded CO shows up. This indicates the formation of small palladium islands on the surface. By comparison with the work on the alumina surface, this means that at this coverage small islands with more than 10 atoms per particle must exist.²⁵ With increasing amount of deposited palladium, these particles grow. At the highest coverage, the whole oxide is covered by palladium islands as stated above. Therefore, the change in the intensity of the absorption bands of CO on palladium is not that large when going to higher Pd coverage. This can be seen from Figure 2 where the intensity of the absorption bands is plotted as a function of the palladium coverage. Investigation of CO adsorption on small palladium particles on a well-ordered Al_2O_3 surface revealed a similar behavior with respect to the habit of the spectra as a function of the size of the particles.^{25,26}

3.2. Influence of Pd Deposition on the Substrate Phonons. Further insight into the growth behavior can be obtained by an investigation of the phonons of the oxide film. Figure 3 shows HREEL spectra of the phonon region of the chromium oxide surface. The phonon spectrum of the clean surface has already

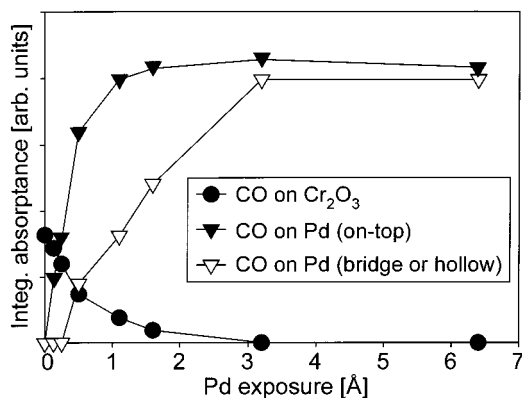


Figure 2. Plot of the integrated absorbance of the CO stretching signal of CO on different adsorption sites derived from the data shown in Figure 1.

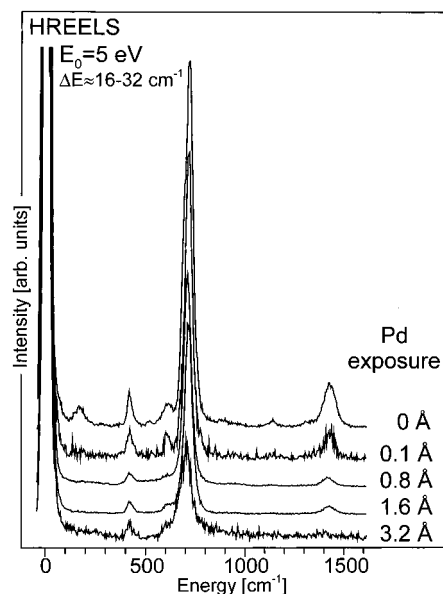


Figure 3. Electron energy loss spectra of the Cr₂O₃(0001)/Cr(110) surface covered with different amounts of Pd at 90 K. The data have been normalized to the elastic signal.

been investigated in detail before.^{9,27} It is dominated by three energy losses at 714, 634, and 417 cm⁻¹ which can be assigned to Fuchs–Kliewer phonons and a further loss at 685 cm⁻¹ which is visible as a shoulder of the main signal. The additional loss at 172 cm⁻¹ is due to a localized “microscopic” surface phonon which is strongly influenced by the presence of adsorbates.²⁷ Upon deposition of palladium, the phonon signal at 172 cm⁻¹ vanishes immediately, whereas the other peaks are attenuated more slowly. At the same time, there is a broadening of the energy losses. However, it is difficult to quantify this broadening, because the intensity of the scattered electrons is rather small because of the roughness of the surface induced by the palladium particles. This causes the electrons to be strongly scattered off the specular direction.²⁸ The count rate of the elastic signal decreases by 2 orders of magnitude, so that for obtaining a reasonable signal-to-noise ratio also, the resolution of the spectrometer had to be decreased.

The more rapid attenuation of the surface phonon at 172 cm⁻¹ is expected because it represents a mode strongly localized in the first layers of the oxide surface.²⁷ As already indicated by the attenuation of the signal of physisorbed CO on the chromium oxide in the infrared spectra, small amounts of palladium seem to influence large parts of the surface, therefore, quenching the surface phonon immediately. The influence of the metallic

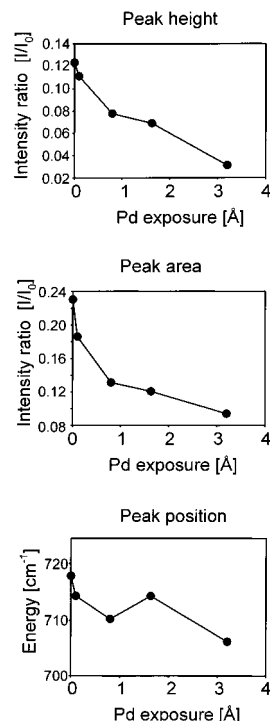


Figure 4. Height, area, and position of the peak of the main Fuchs–Kliewer phonon mode for the 90 K deposits.

overlayer on the intensity of the Fuchs–Kliewer phonons can be described by a model developed by Dubois et al.²⁹ They designed a two layer model consisting of a nonmetallic substrate and a closed metallic overlayer and assumed dipole scattering. The scattered electrons interact with the fluctuations of the electric field at the surface,²⁸ which is produced by the collective excitations of the conduction electrons of the metallic film (plasmons) and the optical substrate phonons. This theory predicts a complete screening of the phonons by a closed metallic overlayer. Additionally, a large background is observed in the HREEL spectra, which only slowly decreases with increasing loss energy. The reason for this is a low-frequency collective mode of the metallic overlayer. Complete screening of the phonons is achieved at a critical film thickness d_c which can be estimated to $d_c = (1/Q_c)(\omega_{TO}/\omega_p)^2(1 + \epsilon_0)$ with Q_c as the maximum wavevector accepted by the spectrometer, ω_{TO} as the frequency of the transversal optical phonon of the substrate, ω_p as the frequency of the bulk plasmon of the metal, and ϵ_0 as the static dielectric constant of the substrate. In the case of palladium deposition on the Cr₂O₃(0001) surface, the critical thickness can be estimated to $d_c = 0.2$ Å, using the following parameters: $\omega_{TO} = 710$ cm⁻¹, $\omega_p = 7$ eV,³⁰ $\epsilon_0 = 11.7$,³¹ $Q_c = 10^6$ cm⁻¹. This shows that a complete layer of palladium (2.2 Å) would completely screen the surface phonons. If one assumes three-dimensional growth, the model provides a minimum diameter $R > 1/Q_c = 100$ Å for holes in the metal film in which the phonons still can propagate.²⁹ If the uncovered parts of the surface are smaller than this value, the phonons are screened and cannot be detected by HREELS.

The intensity of the most intensive phonon mode is reduced to about 1/3 at an average film thickness of 3.2 Å as plotted in Figure 4. In agreement with the results from infrared spectroscopy (see Figures 1 and 2), this demonstrates that the growth mode is not three-dimensional. For classical layer-by-layer growth, the phonon attenuation should be even more pronounced. A growth mode with a high density of islands is a more likely explanation.

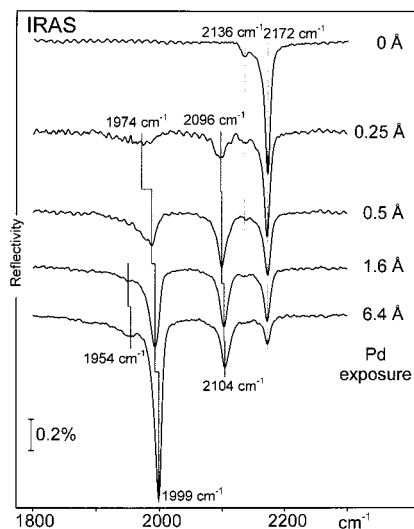


Figure 5. Infrared reflection absorption spectra of 10 L CO adsorbed at 90 K on $\text{Cr}_2\text{O}_3(0001)/\text{Cr}(110)$ as a function of Pd exposure at 300 K.

This is in line with a variety of studies where the growth of metals on oxide surfaces has been the subject to HREELS investigations. Sodium is growing in a layer-by-layer mode on the $\text{Cr}_2\text{O}_3(0001)$ film.^{5,6} This was concluded from the complete attenuation of the phonons at a coverage of 2.2 monolayers. In different systems with layer-by-layer growth mode, complete attenuation was achieved with even smaller amounts of deposited metal.^{29,34,35} On the other hand, if the metal is growing in a three-dimensional mode, the attenuation was reported to be much weaker.^{29,35,36} During the deposition of silver onto a $\text{MgO}(100)/\text{Mo}(100)$ surface, the phonon was detected at coverages up to 10 monolayers.³⁶ The part of the surface which was covered by the silver was estimated to be about 35%.

3.3. Deposition at 300 K. If palladium is deposited at 300 K, the growth behavior is expected to be different. The mobility and the internal energy of the deposited palladium atoms are higher. Pd atoms find and nucleate at sites with higher work of adhesion, and a smaller number of particles are formed which contain more palladium atoms. In the case of palladium particles on aluminum oxide, a deposition temperature of 300 K led to large, crystallographically well-oriented three-dimensional aggregates even at smaller palladium coverages.^{32,33} Figure 5 shows the IR spectra recorded after adsorption of 10 L of CO onto $\text{Cr}_2\text{O}_3(0001)$ onto which palladium was deposited at 300 K. The spectra are remarkably different from the ones obtained for palladium particles deposited at 90 K. Even at high palladium coverages, the absorption band that is due to CO on the chromium oxide is still visible. This points toward a three-dimensional growth mode because the coverage of 6.4 Å palladium corresponds to about three monolayers. Another difference to the growth at 90 K is the fact that the absorption band of the physisorbed CO can be detected up to at least 1.6 Å of palladium. Both bands of CO adsorbed on the chromium oxide do not change in frequency with increasing palladium coverage. This shows that there are large areas which are not covered by metal even at higher Pd deposition.

From the previous discussion, it follows that the height of the aggregates deposited at 300 K is larger for a given amount of palladium than the one of the deposits at 90 K. Already at the lowest amount of deposited palladium (0.25 Å), a signal of bridge-bonded CO shows up in the spectra. This band is nearly as intense as the peak of linearly bonded CO. With increasing coverage, only the band of bridge-bonded CO gains intensity,

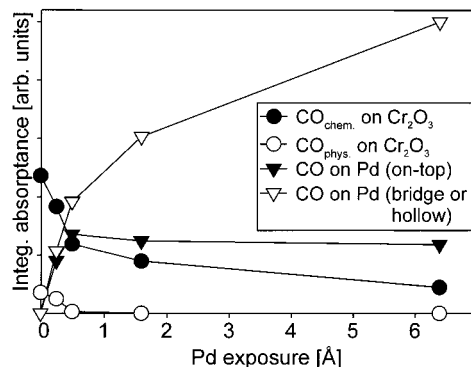


Figure 6. Plot of the integrated absorbance of the CO stretching signal of CO on different adsorption sites derived from the data shown in Figure 5.

whereas the intensity of the linearly bonded CO remains constant. The frequency of the band of the bridge-bonded molecules increases from 1974 to 1999 cm^{-1} , and a second band comes up at 1954 cm^{-1} which is much weaker. The shift of the band of the linearly bonded CO is smaller than in the case of the 90 K deposits. As stated above, the CO molecules prefer bridge sites on larger aggregates at low coverage. The high intensity and the small fwhm of the band at about 2000 cm^{-1} show that the aggregates expose well-ordered facets. Comparison of the frequency of the band at about 2000 cm^{-1} with single-crystal data suggests that Pd(100) or Pd(110) are present.^{37,38} The signal at 1954 cm^{-1} could be associated with CO molecules on (111) facets.³⁹ However, the investigation of the palladium deposits on aluminum oxide has shown that such a one-to-one assignment is not possible. The infrared spectra of CO on this kind of surface show a similar intensity profile in the corresponding region.^{25,26} However, a detailed STM and LEED analysis showed that (111) is the mainly exposed facet especially on large particles.^{32,33} It was argued that “intensity borrowing” gives rise to the high intensity of the mode whose frequency corresponds to adsorption on (110) and (100) facets. Such an explanation is also applicable for the $\text{CO}/\text{Pd}/\text{Cr}_2\text{O}_3(0001)$ system.

The number of adsorption sites for linearly bonded CO seems to be limited as may be deduced from the data in Figure 6. On the small, less ordered particles these sites are preferred.^{25,26} Possibly a certain number of smaller particles exist on the surface even at higher Pd coverage. Their prevalence may be connected with certain defects of the oxide surface.

3.4. Influence on the Substrate Phonons. The difference in growth modes between deposition at 90 and 300 K also manifests itself in the attenuation of the oxide phonons. Figure 7 shows HREEL spectra of the $\text{Cr}_2\text{O}_3(0001)$ surface with different amounts of palladium deposited at 300 K. The intensity of the phonons is smaller than at 90 K because of the higher substrate temperature during the measurement. The number of already excited vibrations is higher due to the higher temperature, and so the loss probability for the electrons is reduced.²⁸ The decrease in intensity of the most intense Fuchs–Kliwer phonon with increasing Pd coverage is much less pronounced as compared with the 90 K deposits. Especially in the low coverage regime, there is a much smaller decrease. This again shows that larger particles are formed and large parts of the oxide surface are not covered with palladium. Even at 6.4 Å Pd, there still is a signal. In an investigation of silver deposition onto a $\text{MgO}(100)/\text{Mo}(100)$ surface, the signal intensity of the phonon of the MgO film could still be observed for 10 monolayers of silver.³⁶ In this case, the silver that covered part

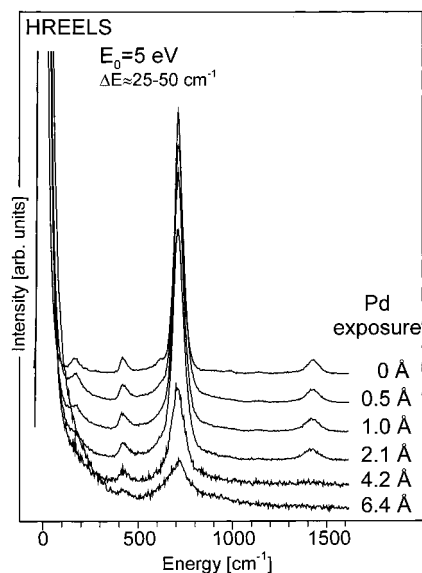


Figure 7. Electron energy loss spectra of the Cr₂O₃(0001)/Cr(110) surface covered with different amounts of Pd at 300 K. The data have been normalized to the elastic signal.

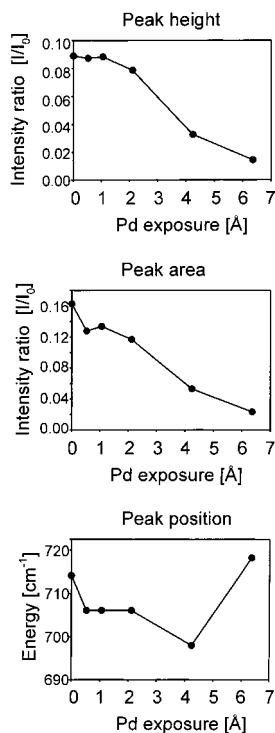


Figure 8. Height, area, and position of the peak of the main Fuchs–Kliwer phonon mode for the 300 K deposits.

of the surface was estimated to be about 35%. In our study, the main Fuchs–Kliwer phonon of the Cr₂O₃(0001) surface is more strongly attenuated for a smaller amount of deposited metal. It seems that the particles which are formed in the present case are rather flat and exhibit a low aspect ratio. Therefore, the fraction of the oxide surface covered by metal is larger leading to a stronger screening of the phonons as compared to the Ag/MgO(100)-system.³⁶

4. Temperature Dependent Structural Changes

4.1. Temperature Programmed Desorption of CO. Figure 9 shows the thermal desorption spectra of CO adsorbed on the Cr₂O₃(0001) surface covered with different amounts of pal-

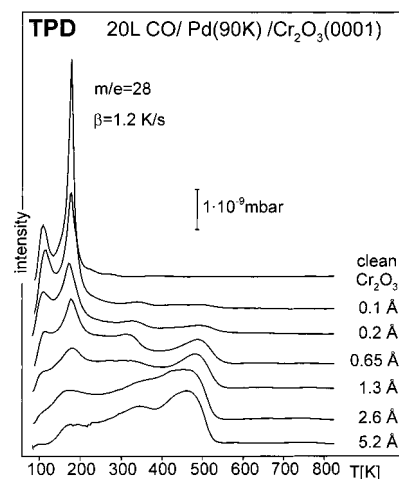


Figure 9. Thermal desorption spectra of 20 L of CO adsorbed on Cr₂O₃(0001)/Cr(110) as a function of Pd exposure at 90 K.

ladium deposited at 90 K. The dose of 20 L corresponds to saturation coverage at the sample temperature of 90 K. On the clean oxide surface, two desorption signals are found at 105 and 170 K which are attributed to a physisorbed and a weakly chemisorbed CO species as discussed above.²⁰ If palladium is deposited onto the oxide surface, the intensity of the desorption signals at 105 and 170 K decreases because of coverage of parts of the surface with palladium. At higher temperatures, several new desorption signals appear which are to be attributed to CO adsorbed on the palladium particles. In the coverage region between 1.3 and 5.2 Å of palladium, the desorption signals of CO on chromium oxide disappear. The disappearance of the signals from physisorbed CO on the oxide at about a monolayer of palladium (2.2 Å) is again an indication of a growth mode with a high density of palladium islands at 90 K as discussed above. At small palladium coverages, two new desorption signals appear at about 340 and 500 K. With increasing palladium coverage, the desorption maximum at 500 K is shifted to lower temperatures, i.e., 460 K. The peak temperature of the signal at 340 K at first shifts to 320 K but then returns to 340 K. Its intensity decreases as compared to the high temperature signal. The spectrum at highest palladium coverage in Figure 9 is similar to the one recorded for a Pd(111) surface⁴⁴ except for the relatively higher signal intensity at around 300–400 K in the spectrum of the present study. However, the differences between the different palladium single-crystal surfaces are small.^{44–46}

The decrease of the peak desorption temperature of the dominating signal from 500 to 460 K indicates a decrease of adsorption energy of the CO. Such a result was also found in the case of palladium particles deposited on a MgO(100) surface⁴⁷ and related to a larger size of the palladium particles. The desorption signal at 340 K could also be detected in previous work on Pd/alumina and was correlated with adsorption on small palladium aggregates.⁴⁸ In TPD spectra of CO from a stepped Pd(112) surface,⁴⁵ also, a quite intense signal at 340 K shows up, suggesting an assignment to step, edge, or corner sites. For small coverages of palladium on the chromium oxide surface, the formation of regular facets is not likely as indicated by the relatively high intensity of the signal at 340 K. Larger particles at higher palladium coverages still do not seem to exhibit a large number of adsorption sites on regular facets as discussed on the basis of the FTIR data above. Correspondingly, the signal at 340 K is intense also for larger Pd deposits, although its fraction of the over-all intensity is reduced. At this

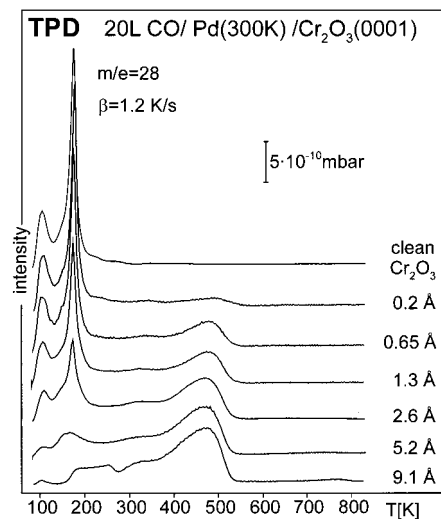


Figure 10. Thermal desorption spectra of 20 L of CO adsorbed on $\text{Cr}_2\text{O}_3(0001)/\text{Cr}(110)$ as a function of Pd exposure at 300 K.

point, one has to note the possibility of morphology changes of the particles in the course of the TDS scan. If morphology changes occur during the scan, the data would not reflect the morphology at the begin of the scan but the different morphologies at the respective temperatures during the scan. As will be shown below, between 90 and 300 K, morphology changes do, indeed, play an important role. Therefore, morphology changes are likely to occur during the TDS scans and modify the spectra as will be discussed below.

Figure 10 shows TDS spectra equivalent to those displayed in Figure 9 but for palladium deposited at 300 K. One difference with respect to the data in Figure 9 is that CO desorption from the uncovered part of the oxide surface vanishes at higher palladium coverages. The corresponding signals disappear between 5.2 and 9.1 Å. This result again demonstrates the different growth modes at 300 K deposition temperature as compared to 90 K. At 300 K the palladium particles are three-dimensional and do not cover the surface fully before several monolayers have been deposited. The desorption of CO from the palladium aggregates is dominated by a signal that shifts from 490 K at low palladium coverage to 470 K at high coverage. This behavior is similar to what was found for the 90 K deposits. The most striking difference to deposition at 90 K is the much weaker desorption intensity between 320 and 340 K in the entire coverage regime. The TDS spectra are even closer to the spectrum of CO on a Pd(111)-surface.⁴⁴ The number of step, edge, and corner sites is obviously smaller,^{45,48} and there are more regular adsorption sites present. This observation is in line with results from infrared spectroscopy. After deposition of palladium, a shoulder can be detected in the desorption signal of CO from the chromium oxide around 160 K, which develops into a clear signal at a coverage of 5.2 Å (see Figure 10). It is possibly due to CO adsorbed at the periphery of the particles. This interpretation is in line with the observation that the signal seems to disappear at higher palladium coverage because then the oxide surface is completely covered so that no peripheral sites exist. The new signal appearing between 200 and 300 K could be observed for both, a Pd(111) single-crystal surface and supported palladium particles.^{32,44}

4.2. Infrared Reflection Absorption Results. Figure 11 shows a series of infrared spectra of CO adsorbed on 3.2 Å palladium deposited at 90 K onto the $\text{Cr}_2\text{O}_3(0001)$ surface and after annealing the system at different temperatures. The two

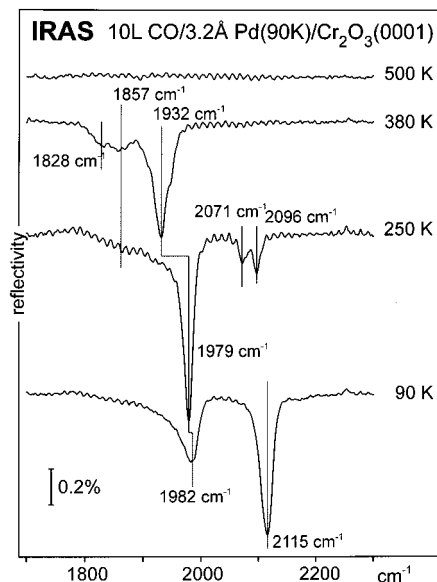


Figure 11. Infrared reflection absorption spectra of 10 L of CO adsorbed at 90 K on the $\text{Cr}_2\text{O}_3(0001)/\text{Cr}(110)$ surface covered with 3.2 Å Pd deposited at 90 K. Afterward, the sample was stepwise annealed at the given temperatures. The spectra were measured after cooling to 90 K.

signals in the spectrum at the bottom (no annealing) can be attributed to CO molecules bound to the palladium particles.^{22–24} The low-frequency signal at 1982 cm^{-1} corresponds to bridge-bonded molecules, whereas the high-frequency band at 2115 cm^{-1} can be assigned to linearly bonded molecules.^{22–24} Upon heating the surface, a fraction of the CO molecules desorbs (see Figure 9). Annealing at 250 K leads to drastic changes in the infrared spectrum. The intensity in the region of the linearly bonded CO is strongly suppressed, and only two small signals at 2071 and 2096 cm^{-1} remain. The band at 2071 cm^{-1} could in principle be assigned to CO molecules which are bound to isolated palladium atoms.^{23,49} However, because palladium deposited at 90 K grows in a layer-by-layer mode, the existence of isolated palladium atoms is rather unlikely even if restructuring had taken place. On a Pd(111) surface, two bands were found in this energy region at a CO coverage between 0.6 and 0.75.³⁹ Therefore, the two signals at 2071 and 2096 cm^{-1} are possibly connected with a specific adsorbate structure at a certain CO coverage. The strong intensity decrease in the region of linearly bound CO is accompanied by an increase of the signal of the bridge-bonded CO molecules. Additionally, the half-width of the latter signal decreases. Assuming that the dynamic dipole moments of the adsorbed CO species did not change during the annealing process, the intensity changes point toward a change of the adsorption sites of the CO molecules. Part of the CO molecules desorbs during the annealing process as is obvious from the desorption peak at 190 K in the corresponding TPD spectrum in Figure 9. In a previous study, it was shown that a small half-width of the infrared signal of bridge-bonded CO molecules on small palladium particles is a sign for good order of the cluster surfaces.^{25,26} Thus, the decrease of the half-width of the peak at 1979 cm^{-1} is an indication that the crystalline order of the cluster increases upon annealing at 250 K. Annealing the surface at 380 K leads to desorption of even more CO. Now also 3-fold hollow sites become accessible while no longer linearly bound CO molecules can be detected.²⁵ The weaker bond of the linearly bound species compared to the bridge and 3-fold hollow bonded molecules was already

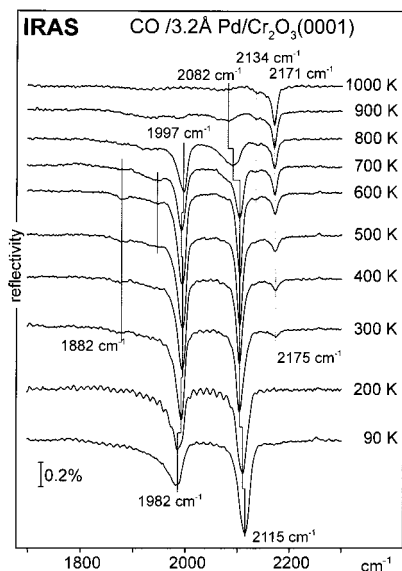


Figure 12. Infrared reflection absorption spectra of 10 L of CO adsorbed at 90 K on the Cr₂O₃(0001)/Cr(110) surface covered with 3.2 Å Pd deposited at 90 K. Afterward, the sample was annealed at the given temperatures. The spectra were measured after cooling to 90 K and saturating the surface with CO.

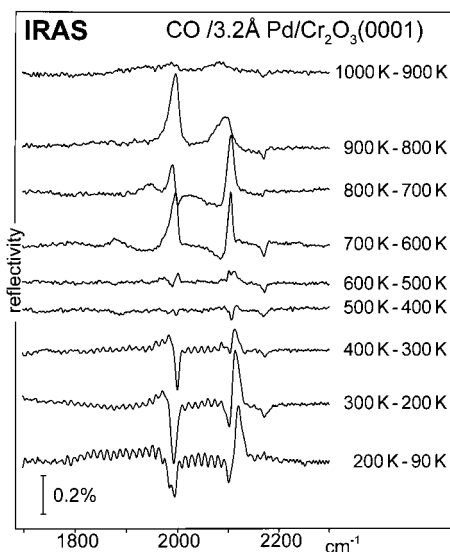


Figure 13. Difference between two successive spectra in Figure 5 as indicated.

discussed in earlier work on supported palladium particles on alumina.^{24,25,50}

To study the temperature dependent changes of the cluster structure for constant CO coverage, a readsorption experiment was carried out. After annealing the CO-covered surface and cooling to 90 K, the surface was again saturated with CO. The spectra in Figure 12 support the interpretation that the particles become more ordered and crystalline upon annealing to 300 K as already discussed above because the absorption bands become narrower. Additionally, the band in the region of the bridge-bonded CO gets more intensive and shifts to higher wavenumbers. The temperature dependence of morphological changes gets more clear from the difference spectra shown in Figure 13. At 400 K, the ordering process has nearly completely finished as is obvious from the nearly vanishing intensity in the difference spectrum. Interestingly, now a band appears at 2175 cm⁻¹ which can be attributed to CO bound to the chromium oxide surface,²⁰ which is another indication for the

restructuring of the palladium particles. The palladium atoms of the clusters have moved away from sites which imply a direct contact to the oxide surface in favor of metal-metal bonds. The diffusion can occur along the oxide surface to an existing particle or from the border of a particle to higher layers.¹ The particles become higher which would be thermodynamically more favored. Another possibility would be a diffusion of palladium into the oxidic substrate. Although this cannot be ruled out completely, it is not very likely because the temperatures are probably not high enough. Pd deposits on a thin alumina film were shown to start diffusion into the substrate at about 400 K⁵¹ but only to a very small extent at that temperature. The changes in the infrared spectra in Figure 5 between 400 and 600 K are rather small, so that a diffusion of the Pd into the chromium oxide film does not seem to take place or if at all only a very small fraction diffuses into the oxide. As will be shown below, such a diffusion is likely to occur at higher temperatures. Another indication for an ordering of the particles is the appearance of a signal at 1882 cm⁻¹. From the different palladium single crystal surfaces studied up to now with respect to CO adsorption, only Pd(111) shows an absorption band in this frequency region at saturation coverage.²² This band is attributed to CO in 3-fold-hollow sites indicating that (111) facets form on the palladium particles.

In several studies of CO adsorption on supported palladium particles, CO dissociation was found although often also the opposite result was reported.² The temperature region for dissociation ranges from 300 to 600 K.⁴⁸ After annealing the CO-covered deposits on the chromium oxide surface to 600 K, the CO molecules are completely desorbed (see Figures 1 and 2). The infrared spectrum after readsorption of CO is only very slightly different from the spectra obtained after annealing at 500 and 400 K. If dissociation of CO had occurred in noticeable amounts adsorption sites would be blocked because of the formation of carbon leading to a decreased coverage after readsorption and thus to smaller absorption signals in the IR spectrum. Because this cannot be observed, it is unlikely that CO dissociation occurs in noticeable amounts.

Apparently, at 90 K, thermodynamic equilibrium is not reached. This is a commonly observed behavior for middle to late transition metals deposited on oxide surfaces.¹ The thermodynamically favored structures are thicker three-dimensional islands which cover only small parts of the oxide surface.¹ The ordering process seems to have finished after annealing at 400 K. Between 400 and 600 K, no changes can be observed.

When the sample is annealed at temperatures of 700 K and higher, significant changes in the infrared spectra of the adsorbed CO occur. The intensity of the signals of CO molecules on the palladium clusters decreases until it nearly completely disappears at 1000 K (see Figures 4 and 5). At the same time, the signals of CO molecules adsorbed on the chromium oxide surface increase. The band at 2134 cm⁻¹ is caused by a weakly bound physisorbed CO species, whereas the band at 2171 cm⁻¹ is due to a more strongly bound chemisorbed species.²⁰ The temperature of the final annealing step after oxide preparation is 1000 K. The CO signal is weaker and broader than on the freshly prepared oxide which indicates that at least parts of the oxide are different from a freshly prepared one. There seems to be no palladium on the surface. Desorption of the palladium can be ruled out because the temperatures are too low.⁵⁴ The apparent explanation is a diffusion of the palladium into the oxide film or even further into the chromium metal. Diffusion of metal deposits into oxide substrates has often been observed.^{41,51,52} From electron spin resonance experiments, it is known that

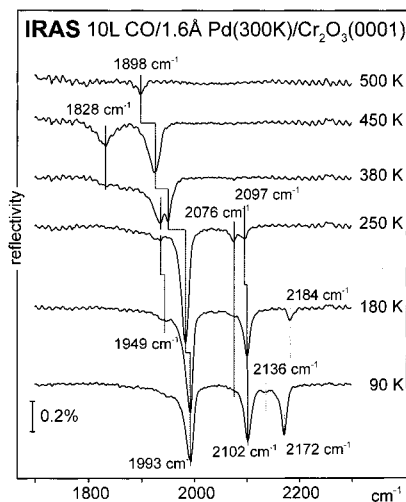


Figure 14. Infrared reflection absorption spectra of 10 L of CO adsorbed at 90 K on the $\text{Cr}_2\text{O}_3(0001)/\text{Cr}(110)$ surface covered with 1.6 Å Pd deposited at 300 K. Afterward, the sample was stepwise annealed at the given temperatures. The spectra were measured after cooling to 90 K.

rhodium and iridium atoms can diffuse into $\alpha\text{-Cr}_2\text{O}_3$.⁵³ It was proposed that diffusion is promoted by defects of the Cr_2O_3 lattice. Defects may also play a role for the diffusion of palladium into the $\text{Cr}_2\text{O}_3(0001)$ film. We know from previous studies⁶ that there is diffusion apparently along grain boundaries.

If palladium is deposited at 300 K, the changes in the infrared spectra of CO are expected to be less pronounced for annealing temperatures below 300 K. At 300 K, the growth mode is different from that at 90 K. The particles are higher and exhibit a better crystallinity. Indeed, annealing of a surface onto which 1.6 Å palladium was deposited at 300 K does not show such significant changes in the region of the bridge-bonded CO upon annealing at temperatures of up to 250 K, as shown in Figure 14. CO molecules adsorbed on the chromium oxide desorb between 180 and 250 K as also indicated by the TPD spectra. The linearly bound CO on the palladium particles desorbs completely below 380 K as also observed for the 90 K deposits. At 250 K there are also two signals in this region. The absorption band of the bridge-bonded CO molecules does not change very much until 250 K as expected. Only a slight increase in intensity can be detected together with a reduction of the half width. However, the changes are much less pronounced than for the 90 K deposits. The absence of strong changes is a sign that the influence of the CO molecules on the morphology of the clusters is only small. The particles which are grown at 300 K are covered with CO at 90 K and then annealed to 300 K again. If the CO had a strong influence on the structure the spectra should reveal stronger changes. It seems that the equilibrium structure which exists between 300 and 600 K is kept once it has developed.

5. Summary

The growth of palladium particles on an $\text{Cr}_2\text{O}_3(0001)/\text{Cr}(110)$ surface at 90 and 300 K was investigated with HREELS and IRAS. At 90 K, palladium probably forms small, flat islands without any well-ordered facets. CO adsorption on the substrate is fully suppressed already at low palladium coverages pointing toward a layer-by-layer growth. This conclusion is corroborated by the strong attenuation of the substrate phonon intensity. In contrast to that, palladium deposited at 300 K forms larger aggregates which exhibit a higher degree of crystallinity.

Although the infrared spectra point toward a three-dimensional growth mode, the attenuation of the oxide phonons indicates that the height of these aggregates is small. They exhibit a low aspect ratio.

The particles grown at 90 K become more ordered upon annealing and exhibit an increased crystallinity. The ordering process finishes at 400 K. Comparison of IR data for clusters deposited at 90 and 300 K indicates that the adsorbed CO molecules do not play a significant role for the ordering process. CO completely desorbs until 550 K and CO dissociation could not be detected. The palladium particles are stable until 600 K. At higher temperatures the palladium diffuses into the oxide film until it is completely removed from the surface.

Acknowledgment. We are grateful to a number of agencies that have supported our work: Deutsche Forschungsgemeinschaft (DFG), Bundesministerium für Bildung, Wissenschaft, Forschung und Technologie (BMBF), and Fonds der chemischen Industrie.

References and Notes

- (1) Campbell, C. T. *Surf. Sci. Rep.* **1997**, *27*, 1.
- (2) Henry, C. *Surf. Sci. Rep.* **1998**, *31*, 231.
- (3) Bäumer, M.; Freund, H.-J. *Prog. Surf. Sci.* **1999**, *61*, 127.
- (4) Freund, H.-J.; Bäumer, M.; Kuhlbeck, H. *Adv. Catal.* **2000**, *45*, 333.
- (5) Ventrice, C. A., Jr.; Ehrlich, D.; Garfunkel, E. L.; Dillmann, B.; Heskett, D.; Freund, H.-J. *Phys. Rev. B* **1992**, *46*, 12892.
- (6) Dillmann, B.; Rohr, F.; Seiferth, O.; Klivenyi, G.; Bender, M.; Homann, K.; Yakovkin, I. N.; Ehrlich, D.; Bäumer, M.; Kuhlbeck, H.; Freund, H.-J.; *Faraday Discuss.* **1996**, *105*, 295.
- (7) Weast, R. C. *CRC Handbook of chemistry and physics*; CRC Press: Boca Raton, FL, 1984.
- (8) Seiferth, O.; Wolter, K.; Dillmann, B.; Klivenyi, G.; Freund, H.-J.; Scarano, D.; Zecchina, A. *Surf. Sci.* **1999**, *421*, 176.
- (9) Kuhlbeck, H.; Xu, C.; Dillmann, B.; Haßel, M.; Adam, B.; Ehrlich, D.; Wohlrab, S.; Freund, H.-J.; Ditzinger, U. A.; Neddermeyer, H.; Neuber, M.; Neumann, M. *Ber. Bunsen-Ges. Phys. Ch.* **1992**, *96*, 15.
- (10) Xu, C.; Dillmann, B.; Kuhlbeck, H.; Freund, H.-J. *Phys. Rev. Lett.* **1991**, *67*, 3551.
- (11) Hemmerich, I.; Rohr, F.; Seiferth, O.; Dillmann, B.; Freund, H.-J. *Z. Phys. Chem.* **1997**, *202*, 31.
- (12) Bender, M.; Yakovkin, I. N.; Freund, H.-J. *Surf. Sci.* **1996**, *365*, 394.
- (13) Di Castro, V.; Furlani, C.; Polzonetti, G. *J. Electron Spectrosc. Relat. Phenom.* **1988**, *46*, 297.
- (14) Wilde, M.; Beauport, I.; Stuhl, F.; Al-Shamery, K.; Freund, H.-J. *Phys. Rev. B* **1999**, *59*, 13401.
- (15) Zhao, W.; Asscher, M.; Wilde, M.; Al-Shamery, K.; Freund, H.-J.; Staemmler, V.; Wieszowska, M. *Phys. Rev. B* **2000**, *62*, 7527.
- (16) Rodriguez, J. A.; Chaturvedi, S.; Kuhn, M.; van Ek, J.; Diebold, U.; Robbert, P. S.; Geisler, H.; Ventrice, C. A., Jr. *J. Chem. Phys.* **1997**, *107*, 9146.
- (17) Rohr, F.; Bäumer, M.; Freund, H.-J.; Mejias, J. A.; Staemmler, V.; Müller, S.; Hammer, L.; Heinz, K. *Surf. Sci.* **1997**, *372*, L291.
- (18) Bender, M.; Ehrlich, D.; Yakovkin, I. N.; Rohr, F.; Bäumer, M.; Kuhlbeck, H.; Freund, H.-J.; Staemmler, V. *J. Phys.: Condens. Matter* **1995**, *7*, 5289.
- (19) Dillmann, B. Ph.D. Thesis, Ruhr-Universität, Bochum, Germany, 1996.
- (20) Pykavy, M.; Staemmler, V.; Seiferth, O.; Freund, H.-J. *Surf. Sci.* **2001**, *479*, 11.
- (21) Hoffmann, F. M. *Surf. Sci. Rep.* **1983**, *3*, 107.
- (22) Tüshaus, M.; Berndt, W.; Conrad, H.; Badshaw, A. M.; Persson, B. *Appl. Phys. A* **1990**, *51*, 91.
- (23) Kündig, E. P.; Moskovits, M.; Ozin, G. A. *Can. J. Chem.* **1972**, *50*, 357.
- (24) Rainer, D. R.; Wu, M.-C.; Mahon, D. I.; Goodman, D. W. *J. Vac. Sci. Technol. A* **1996**, *14*, 1184.
- (25) Wolter, K.; Seiferth, O.; Kuhlbeck, H.; Bäumer, M.; Freund, H.-J. *Surf. Sci.* **1998**, *399*, 190.
- (26) Wolter, K.; Seiferth, O.; Libuda, J.; Kuhlbeck, H.; Bäumer, M.; Freund, H.-J. *Surf. Sci.* **1998**, *402–404*, 428.
- (27) Wolter, K.; Scarano, D.; Fritsch, J.; Kuhlbeck, H.; Zecchina, A.; Freund, H.-J. *Chem. Phys. Lett.* **2000**, *320*, 206.
- (28) Ibach, H.; Mills, D. L. *Electron Energy Loss Spectroscopy and Surface Vibrations*; Academic Press: New York, 1982.

- (29) Dubois, L. H.; Schwartz, G. P.; Camley, R. E.; Mills, D. L. *Phys. Rev. B* **1984**, *29*, 3208.
- (30) Vehse, R. C.; Arakawa, E. T.; Williams, M. W. *Phys. Rev. B* **1970**, *1*, 517.
- (31) Renneke, D. R.; Lynch, D. W. *Phys. Rev. A* **1965**, *2*, 530.
- (32) Bäumer, M.; Libuda, J.; Sandell, A.; Freund, H.-J.; Graw, G.; Bertrams, Th.; Neddermeyer, H. *Ber. Bunsen-Ges. Phys. Chem.* **1995**, *99*, 1381.
- (33) Freund, H.-J. *Angew. Chem., Int. Ed. Engl.* **1997**, *36*, 452.
- (34) Winkelmann, F.; Wohlrab, S.; Libuda, J.; Bäumer, M.; Cappus, D.; Menges, M.; Al-Shamery, K.; Kühlenbeck, H.; Freund, H.-J. *Surf. Sci.* **1994**, *307*, 1148.
- (35) Petrie, W. T.; Vohs, J. M. *J. Chem. Phys.* **1994**, *101*, 8098.
- (36) Schaffner, M.-H.; Patthey, F.; Schneider, W.-D. *Surf. Sci.* **1998**, *417*, 159.
- (37) Ortega, A.; Hoffmann, F. M.; Bradshaw, A. M. *Surf. Sci.* **1982**, *119*, 79.
- (38) Chesters, M. A.; McDougall, G. S.; Pemble, M. E.; Sheppard, N. *Surf. Sci.* **1985**, *164*, 425.
- (39) Tüshaus, M. Ph.D. Thesis, Freie Universität, Berlin, Germany, 1989.
- (40) Berkó, A.; Ménesi, G.; Solymosi, F. *J. Phys. Chem.* **1996**, *100*, 17732.
- (41) Chen, J. G.; Colaianni, M. L.; Weinberg, W. H.; Yates, J. T., Jr. *Surf. Sci.* **1992**, *279*, 223.
- (42) Reference deleted in proof.
- (43) Reference deleted in proof.
- (44) Guo, X.; Yates, J. T., Jr. *J. Chem. Phys.* **1989**, *90*, 6761.
- (45) Ramsier, R. D.; Lee, K.-W.; Yates, J. T., Jr. *Surf. Sci.* **1995**, *322*, 243.
- (46) Behm, R. J.; Christmann, K.; Ertl, G.; Van Hove, M. A. *J. Chem. Phys.* **1980**, *73*, 2984.
- (47) Henry, C. R.; Chapon, C.; Goyhenex, C.; Monot, R. *Surf. Sci.* **1992**, *272*, 283.
- (48) Stará, I.; Matolín, V. *Surf. Sci.* **1994**, *313*, 99.
- (49) Gelin, P.; Siedle, A. R.; Yates, J. T., Jr. *J. Phys. Chem.* **1984**, *88*, 2978.
- (50) Sandell, A.; Beutler, A.; Nyholm, R.; Andersen, J. N.; Andersson, S.; Brühwiler, P. A.; Mårtensson, N.; Libuda, J.; Wolter, K.; Seiferth, O.; Bäumer, M.; Kühlenbeck, H.; Freund, H.-J. *Phys. Rev. B* **1998**, *57*, 13199.
- (51) Sandell, A.; Libuda, J.; Bäumer, M.; Freund, H.-J. *Surf. Sci.* **1996**, *346*, 108.
- (52) Chen, J. G.; Crowell, J. E.; Yates, J. T., Jr. *Surf. Sci.* **1987**, *185*, 373.
- (53) Burlamacchi, L.; Ferino, I.; Marongiu, B.; Torazza, S. *J. Phys. Chem.* **1984**, *88*, 3563.
- (54) Heitzinger, J. M.; Gebhard, S. C.; Parker, D. H.; Koel, B. E. *Surf. Sci.* **1992**, *260*, 151.